

High-pressure structural behavior of α -Fe₂O₃ studied by single-crystal X-ray diffraction and synchrotron radiation up to 25 GPa

PASCAL SCHOUWINK,^{1,*} LEONID DUBROVINSKY,² KONSTANTIN GLAZYRIN,² MARCO MERLINI,⁴
MICHAEL HANFLAND,³ THOMAS PIPPINGER,¹ AND RONALD MILETICH¹

¹Mineralphysik, Institut für Geowissenschaften, Universität Heidelberg, 69120 Heidelberg, Germany

²Bayerisches Geoinstitut, Universität Bayreuth, 95440 Bayreuth, Germany

³ESRF, Boîte Postale 220, 38043 Grenoble, France

⁴Dipartimento di Scienze della Terra, Università degli Studi di Milano, 20133 Milano, Italy

ABSTRACT

In situ X-ray diffraction experiments were carried out at pressures up to 25 GPa on a synthetic hematite (α -Fe₂O₃) crystal using synchrotron radiation in an angle-dispersive setup. Experiments were performed in diamond-anvil cells using neon as a pressure-transmitting medium. Single-crystal diffraction data were collected from omega scans and structural refinements were carried out for 10 pressure points. Bulk and linear incompressibilities were obtained from least-squares fits of refined data to the Eulerian strain based Birch-Murnaghan equation of state. Finite strain analysis suggests a truncation at second order, yielding results of $K_0 = 207(3)$, $K_{a0} = 751(17)$, and $K_{c0} = 492(8)$ for bulk and axial moduli, respectively. The a -axis is about 1.5 times stiffer than the c -axis. Compression of the main structural feature, the FeO₆ octahedra, is quite uniform, with just slight changes of distortion parameters at higher pressures.

Keywords: Compressibility, diamond-anvil cell, hematite, axial anisotropy, Neon pressure medium

INTRODUCTION

The majority of transition metal sesquioxides (M₂O₃; M = Al, Ti, V, Cr, Fe) adopt the corundum structure (space-group symmetry $R\bar{3}c$), forming compounds with great importance in mineralogy and technology due to their electric and magnetic properties. Among these, Fe₂O₃ is particularly relevant to geosciences and solid-state physics as it can be considered an archetype Mott-insulator (Pasternak et al. 1999) and is antiferromagnetic between the Morin temperature (260 K) and the Néel temperature (955 K). Considering that iron is one of the most abundant elements in the Earth's mantle, it is essential to understand in detail the high-pressure as well as high-temperature behavior of iron-bearing compounds as well as that of trivalent iron in general. So far, numerous studies have been conducted on the behavior of Fe₂O₃ at P - T ranges corresponding to mantle conditions, focusing in particular on elucidating the nature of the phase transition and of the controversially discussed high-pressure phase of hematite (Shim et al. 2008; Ono et al. 2004; Ono and Ohishi 2005; Liu et al. 2003; Badro et al. 2002; Rozenberg et al. 2002; Pasternak et al. 1999; Olsen et al. 1991). Less attention has been paid to the detailed structural evolution of the α -phase of Fe₂O₃ (hematite). The existing compressibility studies have been confined to powder diffraction (Rozenberg et al. 2002; Liu et al. 2003) or to the low-pressure regime investigated by single-crystal diffraction in DACs (Wilburn and Bassett 1978; Finger and Hazen 1980; Sato and Akimoto 1979).

Bulk and axial compressibilities have been reported by means of XRD up to 60–70 GPa (Sato and Akimoto 1979; Olsen et al. 1991; Rozenberg et al. 2002; Liu et al. 2003). However, structural high-pressure data were only included by Sato and Akimoto (1979) and Rozenberg et al. (2002), both these studies having been done on powders. Furthermore, it may be questioned if the pressure media used, liquid argon or 4:1 methanol-ethanol mixture, are actually appropriate for the investigated pressure ranges, especially as powder samples respond more sensitively to non-hydrostatic environments and thus generate local stresses. Surprisingly, the only structural single-crystal data on α -Fe₂O₃ at high pressure known to us are those of Finger and Hazen (1980), which were restricted to 5.2 GPa.

The aim of this work is to study the structural evolution of Fe₂O₃ by means of single-crystal X-ray diffraction in the quasi-hydrostatic pressure range of liquid neon, below the phase transition to the Rh₂O₃-II type structure, which has been addressed in another paper (Dubrovinsky et al. 2010). The results are discussed and compared to earlier single-crystal data and powder-diffraction data.

EXPERIMENTAL METHODS

Single crystals of α -Fe₂O₃ used in this study were grown by slow oxidation of pure (99.999%) iron at 1200 °C in a gas-mixing furnace following the procedure given by Chase and Morse (1973). Pressure was generated using a diamond-anvil cell with a half opening angle of 35°, diamond anvils with culet sizes of 300 μ m, tungsten carbide seats as backing plates and a rhenium gasket, preindented to 50 μ m with an initial hole-diameter of 150 μ m. For high-pressure experiments, small crystals of approximate dimensions 15 \times 15 \times 15 μ m³ were selected and tested for their quality using an Oxford Diffraction Xcalibur diffractometer. The chosen sample was then placed in the pressure chamber together with ruby spheres as pressure sensor. Neon was loaded at 1.4 kbar as pressure-transmitting medium to provide quasi-hydrostaticity throughout the pressure range investigated.

* Present address: Laboratoire de Cristallographie, Université de Genève, 24 Quai Ernest Ansermet, CH1211 Geneva 4, Switzerland. E-mail: Pascal.Schouwink@unige.ch

High-pressure angle-dispersive single-crystal X-ray diffraction was performed at ID09a of the European Synchrotron Radiation Facility (ESRF). Diffraction data were collected at a wavelength of 0.4153 Å (29.85 keV) in two-thirds bunch mode (maximum current of 200 mA) and a beam size of roughly $10 \times 10 \mu\text{m}^2$ to avoid gasket shadowing. The crystal-to-detector distance was set to 397.934 mm. Pressure was calculated from the R₁ laser-line fluorescence line of ruby spheres (Mao et al. 1986) and cross checked with diffraction rings of solid neon (Fei et al. 2007); pressures were measured before and after each single-crystal data collection. Data acquisition was conducted by scanning in omega from -30 to 30° at a step size of 0.5° and an exposure time of 2 s/frame. Intensities were collected on a MAR555 flatpanel detector with an active area of 430×350 mm. Data were then processed with the CrysAlis software (Oxford Diffraction 2006) and crystal structures were refined in SHELX-97 (Sheldrick 2008) using the WinGX program system (Farrugia 1999). (CIFs available on deposit¹.)

RESULTS AND DISCUSSION

Bulk modulus and linear incompressibility

Figures 1a and 1b show the evolution of normalized lattice parameters and volume as a function of pressure. In general, if error bars are not included, then e.s.d. values are smaller than symbols. The refinements of four structural parameters, z_{Fe} , x_{O} , and isotropic displacement parameters were based on 41 to 47 unique reflections (with $I > 4\sigma$) obtained after data processing. This gives an average of 10 observations per observed parameter, resulting in satisfactory R1 values of roughly 4%, where R1 is defined as $R1 = \Sigma |F_o| - |F_c| / \Sigma |F_o|$. Values of lattice parameters as well as atom positions are given in Table 1. Figure 1a demonstrates the elastic anisotropy of hematite, comprised of a softer c -axis. The present results are in very good agreement with earlier single-crystal data (Finger and Hazen 1980). However, there is a pronounced discrepancy with existing powder data, most noticeable for the a -axis and especially in data by Rozenberg et al. (2002), a being much stiffer in their case. The same holds for the normalized volumes (Fig. 1b). Finger and Hazen's (1980) results are in perfect agreement with our data while there is deviation in powder data, especially at pressures greater than 20 GPa (considering an extrapolation of the present findings), where most pressure media start to generate non-uniform stress fields and pressure gradients within the sample. Bulk and linear incompressibilities were extracted from fitting a third-order Birch-Murnaghan equation of state (Birch 1947) to high-pressure data

$$P = 3K_0 f_E (1 + 2f_E)^{5/2} \left[1 + \frac{3}{2} (K' - 4) f_E + \frac{3}{2} \left(K_0 K'' + (K' - 4)(K' - 3) + \frac{35}{9} \right) f_E^2 \right]$$

where P , K_0 , and K' are pressure, isothermal bulk modulus, and the pressure derivative of K_0 , respectively, and the Eulerian strain f_E equals $[(V/V_0)^{2/3} - 1]/2$. Throughout the following text, K' will

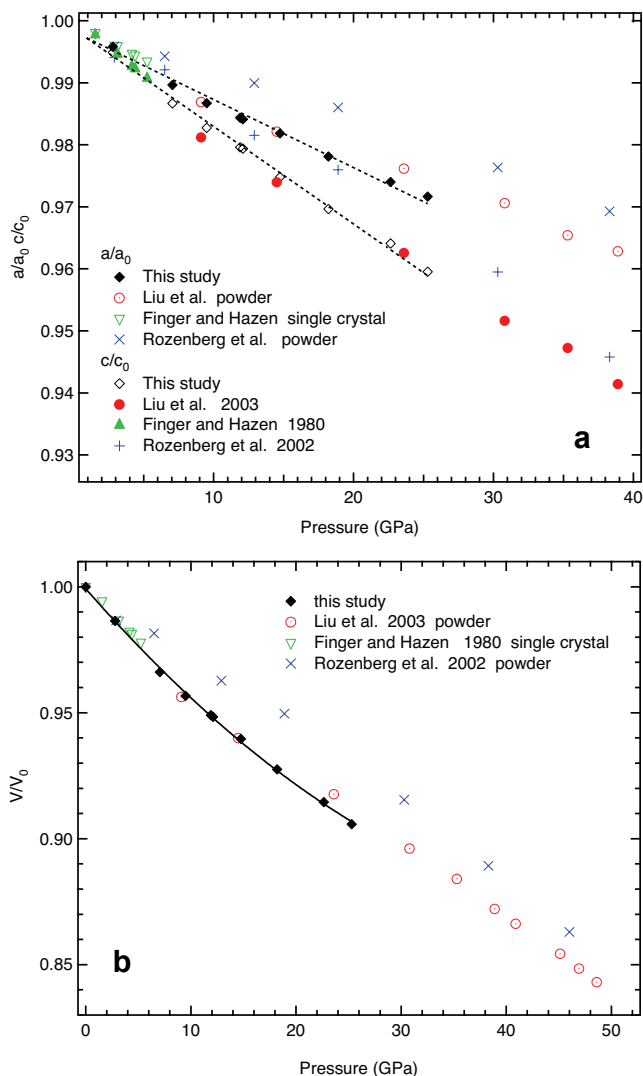


FIGURE 1. Normalized lattice parameters (**a**) unit-cell volume (**b**) as function of pressure. The solid line represents a fit of a second-order Birch-Murnaghan equation of state (see text for details) to the data points determined in this study. Present results agree well with earlier single-crystal data. The e.s.d. values of lattice parameters and pressure (as determined by ruby fluorescence as well as from solid neon diffraction) are smaller than symbols if not indicated otherwise. (Color online.)

¹ Deposit item AM-11-056, CIFs. Deposit items are available two ways: For a paper copy contact the Business Office of the Mineralogical Society of America (see inside front cover of recent issue) for price information. For an electronic copy visit the MSA web site at <http://www.minsocam.org>, go to the *American Mineralogist* Contents, find the table of contents for the specific volume/issue wanted, and then click on the deposit link there.

TABLE 1. Refined structural parameters of α -Fe₂O₃ at various pressures

Pressure (GPa)	a (Å)	c (Å)	V (Å ³)	z_{Fe}	x_{O}	R1 (%)
1e-05	5.0354(17)	13.7477(48)	301.88(2)	0.3552(1)	0.3059(5)	3.79
2.8(2)	5.0160(1)	13.6851(7)	298.19(2)	0.3553(1)	0.3074(8)	2.73
7.1(2)	4.9849(2)	13.5721(8)	292.07(1)	0.3556(1)	0.3074(10)	4.74
9.5(1)	4.9702(3)	13.518(1)	289.24(4)	0.3555(1)	0.3064(9)	2.28
11.9(2)	4.9583(4)	13.475(2)	286.89(5)	0.3555(1)	0.3085(8)	4.23
12.1(2)	4.9571(4)	13.472(2)	286.69(5)	0.3556(1)	0.3068(10)	4.31
14.8(3)	4.9456(4)	13.409(2)	284.03(6)	0.3556(1)	0.3064(10)	2.25
18.2(1)	4.9268(7)	13.338(4)	280.4(1)	0.3559(1)	0.3073(13)	4.05
22.7(2)	4.9116(15)	13.261(8)	277.1(2)	0.3561(3)	0.3067(18)	4.56
25.3(3)	4.8943(15)	13.199(8)	273.8(2)	0.3559(2)	0.3063(13)	4.83

refer explicitly to the derivative of the zero-pressure value of the bulk modulus, K_0 . To estimate the importance of higher order terms and judge the correctness of truncation of the equation of state at a given order, we plotted normalized stress F_E against Eulerian strain f_E in finite strain analysis (Angel 2000), where F_E is defined as $P/3f_E(1 + 2f_E)^{5/2}$. Here the slope of a linear fit is equal to $3K_0(K' - 4)/2$; assessment of this plot (Fig. 2) suggests that it is still reasonable to truncate at second order and thus fixing K' to 4, as was done in most previous studies. Nevertheless it is justifiable to free K' in least squares, as the slope gives a value of $K' = 4.5$. Fits were thus performed both for a truncation at second as well as at third order, the extracted bulk and axial moduli are shown in Table 2. We obtain a K_0 of 207(3) GPa for a weighted fit with fixed K' . This is in excellent agreement with previously published XRD and ultrasonic data shown in Table 2. Parameters given by Finger and Hazen (1980) are slightly higher, which may be owed to the restricted pressure range of their studies, but the pressure dependence of their single-crystal data are in good agreement with ours (Figs. 1a and 1b). Rozenberg et al. (2002) observed a zero-pressure bulk modulus, which is significantly higher, also reflected in the less pronounced slope of the equation of state through their data (Fig. 1b). Their volume data show a strange increase in bulk modulus followed by an

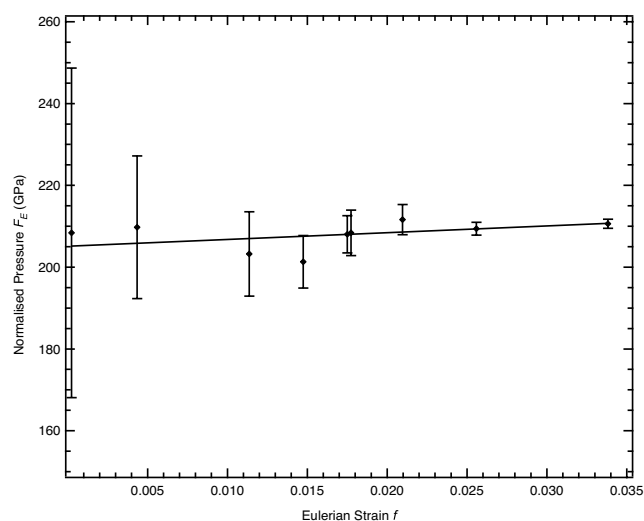


FIGURE 2. Normalized pressure as function of Eulerian strain in the F_E - f plot of Fe₂O₃ of this study. The solid line is a linear fit showing just a very minor slope. The scattering of data points may be explained by inexact repositioning of the DAC after pressure cycling.

enhanced compressibility at pressures greater than 20 GPa where the mentioned quasi-hydrostatic regime of Ar pressure medium is obviously exceeded. Enhanced compressibility may also be due to the onset of the phase transition to the high-pressure phase of Fe₂O₃, designated HP2. In determining equations of state, one must take special care to avoid including instabilities such as arising from softening or distortion of individual lattice parameters. This may bias the results obtained, and different approaches are required to include additional terms, which account for structural evolution throughout the transition (Tröster et al. 2002).

For a weighted fit to a third-order Birch-Murnaghan equation of state we obtain a slightly lower K_0 of 199(8) and a K' of 5.3(9). On one hand this value of K' confirms the inspection of the finite strain analysis, which suggested a value of 4.5. This indicates that the pressure derivative of the bulk modulus may be larger than 4. The same trend was observed by Liu et al. (2003, see Table 2). However, e.s.d. values do increase when truncating at third order. Data scattering may be caused by inexact repositioning of the DAC along the beam after pressure cycling. This results in larger standard deviations due to strong correlation during least-squares fitting. Furthermore, this increase is particularly pronounced for the axial elastic moduli. Assuming $K' = 4$ the fits to our data yield a K_{a0} of 751(17) GPa and a K_{c0} 492(8) GPa, which is close to Liu et al. (2003, Table 2). The c -axis obtained from the present results seems to be slightly stiffer than theirs though, the elastic anisotropy here reflected in c being 1.5 times more compressible than a . Expanding the equation of state to third-order results in a much lesser goodness of fit, leading to the conclusion that a second-order truncation is most likely more appropriate.

Structural change with pressure

The elastic anisotropy of 65% results in the decrease of the c/a ratio with pressure. The trigonal corundum-type structure can be described by two structural parameters, namely the two atom positions not constrained by site symmetry, z_{Fe} and x_O . The structure consists of distorted hexagonal close packing (HCP) of oxygen ions with Fe atoms occupying two-thirds of the octahedral cavities. FeO₆ octahedra form layers perpendicular to the HCP packing direction, c : the unit cell is six layers high. Intra-layer connectivity is established by sharing three common edges, while octahedra from adjacent layers are connected via shared faces in (0001), resulting in Fe₂O₆-dimers along [0001].

The atomic parameters from refinements of the hematite single-crystal of this study are given in Table 1. Atomic positions remain essentially constant throughout the reported pressure

TABLE 2. Isothermal bulk moduli K_0 and axial incompressibilities K_{i0} of α -Fe₂O₃, as extracted from fitting a Birch-Murnaghan equation of state to high-pressure data

K_0 (GPa)	K'	K_{a0}	$K_{a'}$	K_{c0}	$K_{c'}$	Pressure range (GPa)	Reference
207(3)	4.0	751(17)	4.0	492(8)	4.0	$P < 25.3$	This study
199(8)	5.3	628(39)	8.4(1.2)	510(19)	3.6(0.7)	$P < 25.3$	This study
206(5)	4.0	750(18)	4.0	456(21)	4.0	$P < 50$	Liu et al. (2003)
202(4)	4.3(0.3)					$P < 50$	Liu et al. (2003)
258(6)	4.0					$P < 76$	Rozenberg et al. (2002)
225(5)	4.0					$P < 5$	Finger and Hazen (1980)
231	4.0					$P < 3$	Sato and Akimoto (1979)
178	4.0					$P > 3$	Sato and Akimoto (1979)
199(6)	4.0					$P < 11.5$	Wilburn and Bassett (1978)
202.7	4.0					ultrasonic	Liebermann and Schreiber (1968)

Note: Pressure derivatives K' not fixed to 4.0 (rows 2 and 4) are given for a truncation at third order, no axial data were reported by Liu et al. (2003).

range in accordance with most previous studies and thus follow the same trend as other isostructural M₂O₃ compounds, not approaching the ideal HCP lattice. Only Rozenberg et al. (2002) reported a significant increase up to 50 GPa for x_0 . Standard deviations of oxygen atom positions are of course slightly higher than those of the position occupied by the heavier iron atom, and increase with pressure as R1 does likewise. The c/a ratio, which is 2.833 for an ideal HCP corundum-type structure decreases with pressure as has been observed consistently by all previous studies and may induce modifications in the electronic structure of the cation, leading to potential electronic or structural instabilities as is the case for other sesquioxides (Cox 1992). This also may be the origin of the insulator-metal-transition in hematite at pressures of approximately 50 GPa (Pasternak et al. 1999).

Due to the Coulomb repulsion arising from Fe··Fe interaction along the [0001] direction across the shared face of the octahedral dimer unit, the three Fe-O bonds to the shared face of the octahedron [denoted Fe-O(F) here] are considerably longer (2.8926 Å at 1 bar) than those to the unshared face [= Fe-O(E): 2.1155 Å]. This leads to a distortion of the polyhedron as well as a significantly smaller O-Fe-O angle (78° vs. 102°) on the face-sharing side. There exist various parameters, which describe polyhedral distortions (Balić-Žunić 2007; Hazen 1988). Here we report $D_{\text{Fe-O}}$, which is a measure for the degree of distortion of the octahedron, as well as the bond angle variance $\Delta\theta$,

$$\Delta\theta = \frac{\sum_{j=1}^n (\theta_j - \theta_i)^2}{n-1}$$

$$D_{\text{Fe-O}} = (d_{\text{Fe-O(F)}} / d_{\text{Fe-O(E)}} - 1)$$

where θ_j is the observed angle O-M-O between central atom and ligands and θ_i is the ideal angle for the respective polyhedron, 90° for FeO₆, n is the coordination number. $d_{\text{Fe-O(F)}}$ is the bond distance between iron and oxygen atoms from shared faces (top plane), $d_{\text{Fe-O(E)}}$ the distance to oxygen atoms from shared edges (basal plane). In our sample, there is a nearly linear decrease of the mean interatomic distances (Fig. 3). The pressure dependency of Fe-O and Fe-Fe distances is given in Figures 4a and 4b, and values are reported in Table 3. The plots presented in Figures 4a and 4b suggest a slight deviation from linearity at pressures between 3 and 9 GPa. However, data coverage is not dense enough to allow for any conclusions concerning this. Linear compressibilities were determined from linear least-squares fitting using the relationship $\beta R_{ij} = -1/R_{ij(0)} \times dR_{ij}/dP$, slopes dR_{ij}/dP . Bonds Fe-O(F) and Fe-O(E) show very similar compressibilities within the observed pressure range of 0.00131(15) for Fe-O(F) and 0.00126(9) GPa⁻¹ for Fe-O(E) bonds. A virtual compressibility of inter- and intra-layer Fe-Fe distances was also calculated resulting in 0.001194(18) for intra-layer Fe-Fe(E) and 0.001406(8) GPa⁻¹ for distances between iron atoms of adjacent face-sharing octahedral Fe-Fe(F) in direction [000]. This leads to a slight increase in degree of Fe-Fe bond distortion, whereas there is virtually no change for Fe-O bonding, which is contradictory to Rozenberg et al. (2002) but in good agreement with data published by Finger and Hazen (1980), though their pressure range ($P < 5$ GPa) investigated does not unambiguously allow for any conclusions (Fig. 5). As Fe-Fe distances seem to decrease

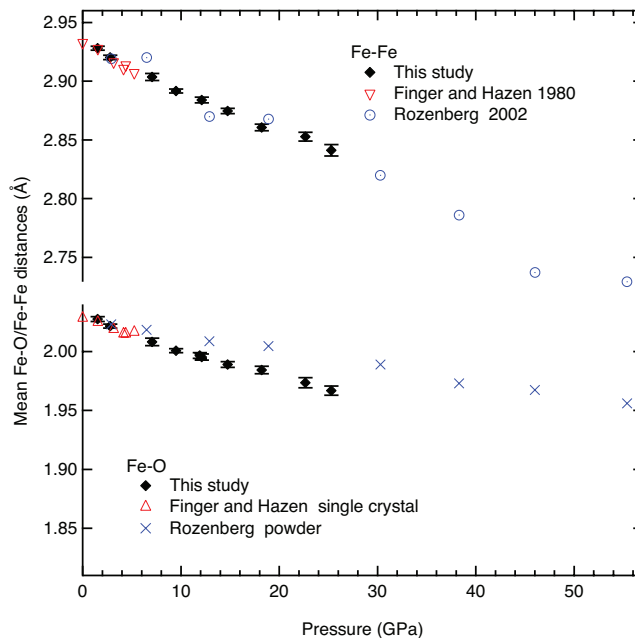


FIGURE 3. Representative mean interatomic distances as function of pressure: mean distances between the central iron atom and oxygen ligands in octahedral environment (**bottom**); mean iron-iron distances between adjacent octahedra (intra- and interplanar, see text). (Color online.)

quicker between face-shared octahedral than face-sharing Fe-O(F) bonds, the O-Fe-O angle (*cis*-position) for oxygen atoms belonging to octahedral faces lying in (000) must increase with pressure to allow the Fe⁺³ ions to get closer to each other in this direction, which is the case, as it is also for the angle to oxygen atoms lying in the basal plane. At the same time the remaining angles having their angle bisector in the (000) plane, as well as the O-Fe-O angle between *trans*-ligands, decrease (Table 3). Due to this compensation between decreasing and increasing angles the octahedral angle variance $\Delta\theta$ remains basically constant. This again is in contradiction to the earlier structural data (Fig. 6).

The cause for Fe-Fe distances decreasing in a more substantial way between face-sharing octahedra than the lateral Fe-Fe distance within the layer, is probably the intra-planar high packing density (000), this two-dimensional framework makes the whole structure more stable in this direction. This also accounts for the high rigidity of M₂O₃ compounds, the c -axis is supported by Coulomb repulsion of face-sharing of octahedral dimers, while the a -axis is stabilized by HCP layers of oxygen atoms. So, on compression there are two competing repulsive mechanisms. High atomic density in (000) seems to be the more significant opposing force, resulting in breakdown of electron correlation as reported elsewhere (Pasternak et al. 1999; Rozenberg et al. 2002; Shim et al. 2008 and references therein). To clarify this point, O-O bonds were examined as well regarding their bond distance as a function of pressure. Bonds with their vectors perpendicular to c , namely those in the top and basal planes of the octahedron, are significantly less compressible, with mean compressibilities of 0.00110(15) GPa⁻¹, than those belonging to shared edges and vertices, with 0.00138(14) GPa⁻¹. This, of course, again reflects the softer c -axis. Bonds within the top and

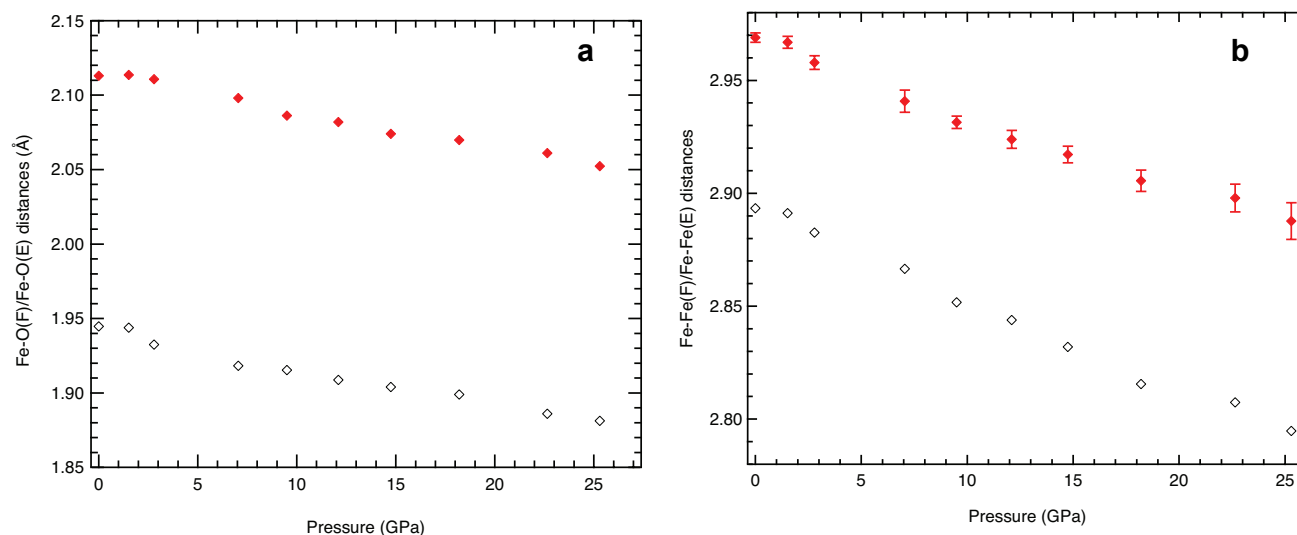


FIGURE 4. Evolution of iron-oxygen distances with pressure shown in **a**. Distances from central iron atom to oxygen atoms belonging to shared faces are denoted Fe-O(F). Evolution of iron-iron distances with pressure (**b**). Distances Fe-Fe(F) (**top**) correspond to face-sharing octahedra, distances Fe-Fe(E) (**bottom**) correspond to iron-iron distances between octahedra within the same (000 l)-plane (see text for details). e.s.d. values are smaller than symbols if not indicated otherwise (see text for details). (Color online.)

TABLE 3. Bond distances (Å), volumes (Å³), and O-Fe-O angles of FeO₆ octahedra of hematite at different pressures

P (GPa)	0.0001	2.8	7.1	9.5	12.1	14.8	18.2	22.7	25.3
Fe-O(F)	2.113(2)	2.111(2)	2.098(4)	2.086(2)	2.082(3)	2.074(3)	2.070(4)	2.061(5)	2.052(6)
Fe-O(E)	1.945(2)	1.933(1)	1.918(3)	1.915(1)	1.909(2)	1.904(2)	1.899(3)	1.886(3)	1.881(2)
<Fe-O>	2.029(2)	2.022(2)	2.008(4)	2.001(2)	1.996(3)	1.989(3)	1.985(4)	1.974(4)	1.967(4)
Fe-Fe(F)	2.893(2)	2.883(3)	2.867(5)	2.851(3)	2.844(4)	2.832(4)	2.816(5)	2.807(6)	2.795(8)
Fe-Fe(E)	2.969(1)	2.958(1)	2.941(1)	2.931(6)	2.924(1)	2.918(1)	2.906(1)	2.898(2)	2.888(2)
<Fe-Fe>	2.931(1)	2.921(2)	2.904(3)	2.891(5)	2.884(2)	2.875(2)	2.861(3)	2.853(3)	2.842(3)
V FeO ₆ (Å ³)	10.74(2)	10.63(1)	10.40(1)	10.30(1)	10.21(1)	10.11(1)	10.00(1)	9.85(2)	9.75(2)
O-Fe-O ^a	78.28(9)	78.49(9)	78.44(16)	78.42(10)	78.48(13)	78.51(11)	78.46(16)	78.71(22)	78.62(25)
O-Fe-O ^b	102.54(5)	102.53(5)	102.71(9)	102.73(5)	102.76(8)	102.86(7)	102.92(9)	103.1(1)	103.12(9)
O-Fe-O ^c	86.04(3)	86.07(3)	85.95(5)	85.9(3)	85.87(4)	85.77(5)	85.68(5)	85.62(8)	85.54(7)
O-Fe-O ^d	90.50(6)	90.30(6)	90.2(1)	90.28(6)	90.21(9)	90.16(8)	90.2(1)	89.9(1)	89.96(1)
O-Fe-O ^e	162.24(9)	162.4(1)	162.3(9)	162.2(1)	162.2(1)	162.1(1)	162.0(2)	162.1(2)	161.9(3)

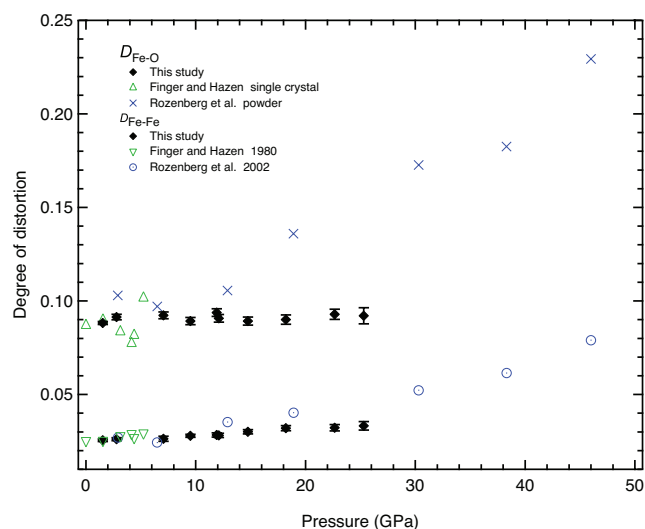


FIGURE 5. Degree of octahedral distortion (see text for details) as function of pressure. Virtually no change with pressure points to a rather uniform compression of FeO₆ octahedra. (Color online.)

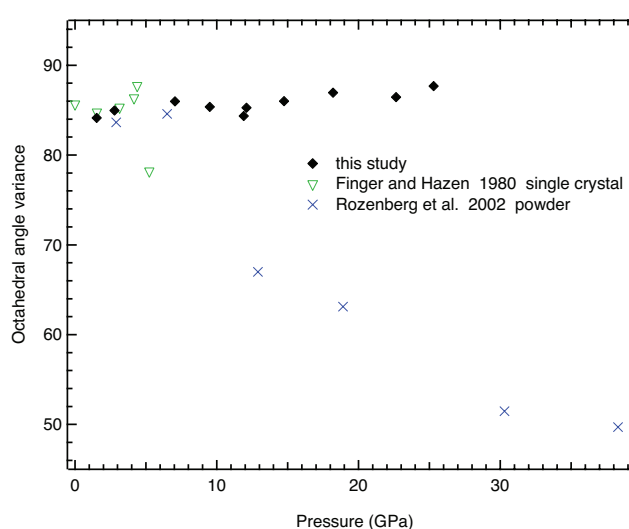


FIGURE 6. Octahedral angle variance as a function of pressure (see text for details). (Color online.)

basal planes actually show hardly any difference at all regarding their elastic behavior $\beta R_{O-O(F)} = 0.00101(12)$ vs. $\beta R_{O-O(E)} = 0.00119(16)$, which is surprising since one would assume, from rigid body theory, that a shared face is far less compressible than an unshared one. The overall stability of the HCP planes seems to dominate the enhanced stiffness of *a* here. This result strongly contradicts data from Rozenberg et al. (2002). In their observation, the octahedron is virtually flattened in *c* direction, with triangular areas of shared faces and thus O-O(F) bonds in fact getting larger with pressure, resulting in a larger face area than the basal plane (unshared), as if O-O bonds in shared faces were to break up. This may be a strong indication of uniaxial stress and non-hydrostatic stress in powder experiments. The present study suggests a uniform compression of the octahedron with respect to the investigated pressure range up to 25.3 GPa, based on hardly existent changes in distortion parameters.

This point is emphasized by the determined octahedral bulk modulus of FeO₆ calculated from values given in Table 3, which is virtually the same as for the bulk structure with $K'_{FeO_6,0} = 4$ and $K_{FeO_6,0} = 204(9)$. This indicates a quite uniform compression mechanism, considering that there is basically no difference within errors between bulk and polyhedral incompressibilities. Compressibility of iron-oxygen octahedra in hematite compares well with that of FeO₆ octahedra in GdFeO₃ (Ross et al. 2004), which do not share faces and have a polyhedral bulk modulus of 188(10). However, it is considerably higher than that of FeTiO₃ and CaFeSi₂O₆, reported values being 140(10) (Wechsler and Prewitt 1984) and 149(4) (Zhang et al. 1997), respectively, but lower than the FeO₆-polyhedral bulk modulus of the amorphous phase of garnet Y₃Fe₅O₁₂ with 260(15) (Gavriliuk et al. 2006). Differences are mainly due to varying mean Fe-O distances as well as connectivities of octahedra.

ACKNOWLEDGMENTS

We acknowledge European Synchrotron Radiation Facility (ESRF) for providing the beamtime (ID09a) this project was conducted on. The work is supported by the Deutsche Forschungsgemeinschaft (DFG) in the project SPP1236.

REFERENCES CITED

- Angel, R.J. (2000) Equations of state. In R.M. Hazen and R.T. Downs, Eds., *High-Temperature and High-Pressure Crystal Chemistry*, 41, p. 35–60. Reviews in Mineralogy and Geochemistry, Mineralogical Society of America, Chantilly, Virginia.
- Angel, R.J., Bujak, M., Zhao, J., Gatta, G.D., and Jacobsen, S.D. (2007) Effective hydrostatic limits of pressure media for high-pressure crystallographic studies. *Journal of Applied Crystallography*, 40, 26–32.
- Badro, J., Fiquet, G., Struzhkin, V.V., Somayazulu, M., Mao, H., Shen, G., and Le Bihan, T. (2002) Nature of the high-pressure transition in Fe₂O₃ hematite. *Physical Review Letters* 89, 20, 205504.
- Balić-Žunić, T. (2007) Use of three-dimensional parameters in the analysis of crystal structures under compression. In Grzechnik, A., Ed., *Pressure-induced Phase Transitions*, p. 157–184. Transworld Research Network, Kerala, India.
- Birch, F. (1947) Finite elastic strain of cubic crystals. *Physical Review B*, 71, 809–824.
- Chase, A.B. and Morse, F.L. (1973) Habit of Fe₂O₃ grown from Na₂B₄O₇. *Journal of Crystal Growth*, 19, 18–20.
- Cox, P.A. (1992) *Transition Metal Oxides*, Clarendon, Oxford.
- Dubrovinsky, L., Boffa-Ballaran, T., Glazyrin, K., Kurnosov, A., Frost, D., Merlini, M., Hanfland, M., Prakapenka, V.B., Schouwink, P., Pippinger, T., and Dubrovinskaja, N. (2010) Single-crystal X-ray diffraction at megabar pressures and temperatures of thousands degrees. *High Pressure Research*, 30, 620–633.
- Farrugia, L.J. (1999) *WinGX* suite for small-molecule single-crystal crystallography. *Journal of Applied Crystallography*, 32, 837–838.
- Fei, Y., Ricolleau, A., Franck, M., Mibe, K., Shen, G., and Prakapenka, V. (2007) Toward an internally consistent pressure scale. *Proceedings of the National Academy of Sciences*, 104, 9182–9186.
- Finger, L.W. and Hazen, R.M. (1980) Crystal structure and isothermal compression of Fe₂O₃, Cr₂O₃, V₂O₅, up to 50kbars. *Journal of Applied Physics*, 51, 55362–55367.
- Gavriliuk, A.G., Struzhkin, V.V., Lyubutin, I.S., Eremets, M.I., Trojan, I.A., and Artemov, V.V. (2006) Equation of state and high-pressure irreversible amorphization in Y₃Fe₅O₁₂. *JETP Letters*, 83, 37–41.
- Hazen, R.M. (1988) A useful fiction: polyhedral modelling of mineral properties. *American Journal of Science*, 288-A, 242–269.
- Klotz, S., Chervin, J.-C., Munsch, P., and Le Marchand, G. (2009) Hydrostatic limits of 11 pressure transmitting media. *Journal of Physics D: Applied Physics*, 42, 075413.
- Liebermann, R.C. and Schreiber, E. (1968) Elastic constants of polycrystalline hematite as a function of pressure up to 3 kilobars. *Journal of Geophysical Research*, 73, 6585–6590.
- Liu, H., Caldwell, W.A., Benedetti, L.R., Panero, W., and Jeanloz, R. (2003) Static compression of α -Fe₂O₃: linear incompressibility of lattice parameters and high-pressure transformations. *Physics and Chemistry of Minerals*, 30, 582–588.
- Mao, H.K., Xu, J., and Bell, B.M. (1986) *Journal of Geophysical Research*, 91, 4673–4676.
- Olsen, J.S., Cousins, C.S., Gerward, L., Jhans, H., and Sheldon, B.J. (1991) A study of the crystal structure of Fe₂O₃ in the pressure range up to 65 GPa using synchrotron radiation. *Physica Scripta*, 43, 327–330.
- Ono, S. and Ohishi, Y. (2005) In situ X-ray observation of phase transformation in Fe₂O₃ at high pressures and high temperatures. *Journal of Physics and Chemistry of Solids*, 66, 1714–1720.
- Ono, S., Kikegawa, T., and Ohishi, Y. (2004) High-pressure phase transition of hematite, Fe₂O₃. *Journal of Physics and Chemistry of Solids*, 65, 1527–1530.
- Oxford Diffraction (2006) *CrysAlis 1.171.33.41*, Oxford Diffraction Ltd., Abingdon, Oxfordshire.
- Pasternak, M.P., Rozenberg, G.K., Machavariani, G.Y., Naaman, O., Taylor, R.D., and Jeanloz, R. (1999) Breakdown of the Mott-Hubbard state in Fe₂O₃: A first-order insulator-metal transition with collapse of magnetism at 50 GPa. *Physical Review Letters*, 82, 4663–4666.
- Ross, N.L., Zhao, J., and Angel, R.J. (2004) High-pressure structural behavior of GdAlO₃ and GdFeO₃ perovskites. *Journal of Solid State Chemistry*, 177, 3768–3775.
- Rozenberg, G.K., Dubrovinsky, L.S., Pasternak, M.P., Naaman, O., Bihan, T.L., and Ahuja, R. (2002) High-pressure structural study of hematite Fe₂O₃. *Physical Review B*, 65, U122–U129.
- Sato, R. and Akimoto, S. (1979) Hydrostatic compression of four corundum-type compounds: α -Al₂O₃, V₂O₅, Cr₂O₃, α -Fe₂O₃. *Journal of Applied Physics*, 50, 5285–5291.
- Sheldrick, G.M. (2008) A short history of SHELX. *Acta Crystallographica*, A64, 112–122.
- Shim, S.-H., Bengtson, A., Morgan, D., Sturhahn, W., Catali, K., Zhao, J., Lerche, M., and Prakapenka, V. (2008) Electronic and magnetic structures of the postperovskite-type Fe₂O₃ and implications for planetary magnetic records and deep interiors. *Proceedings of the National Academy of Sciences*, 106, 14, 5508–5512.
- Tröster, A., Schranz, W., and Miletich, R. (2002) How to couple Landau Theory to an Equation of State. *Physical Review Letters*, 88, 055503.
- Wechsler, B.A. and Prewitt, C.T. (1984) Crystal structure of ilmenite (FeTiO₃) at high temperature and high pressure. *American Mineralogist*, 69, 176–185.
- Wilburn, D.R. and Bassett, W.A. (1978) X-ray diffraction compression studies of hematite under hydrostatic, isothermal conditions. *Journal of Geophysical Research*, 83, 3509–3512.
- Zhang, L., Ahsbahs, H., Hafner, S., and Kutoglu, A. (1997) Single-crystal compression and crystal structure of clinopyroxene up to 10 GPa. *American Mineralogist*, 82, 245–258.

MANUSCRIPT RECEIVED DECEMBER 29, 2010
 MANUSCRIPT ACCEPTED JUNE 27, 2011
 MANUSCRIPT HANDLED BY WENDY MAO